PALEOCEANOGRAPHY, VOL. 14, NO. 6, PAGES 706-715, DECEMBER 1999

Environmental control on Mediterranean salinity and $\delta^{18}O$

Eelco J. Rohling
School of Ocean and Earth Science, Southampton University, Southampton Oceanography Centre, Southampton, England

Abstract. A box model is presented to simulate changes in Mediterranean long-term average salinity and $\delta^{18}O$ over the past 20,000 years. Simulations are validated by comparison with observations. Sensitivity tests illustrate robustness with respect to the main assumptions and uncertainties. The results show that relative humidity over the Mediterranean remained relatively constant around 70%, apparently narrowly constrained to the lower end of the range observed globally over sea surfaces by the basin's land-locked character. Isotopic depletion in run off, relative to the present, is identified as the main potential cause of depletions in the Mediterranean $\delta^{18}O$ record. Also, slight increases in relative humidity (of the order of 5%) might have caused very pronounced isotopic depletions, such as that in sapropel S5 of the penultimate interglacial maximum. The model shows distinctly non proportional responses of $\delta^{18}O$ and salinity to environmental change, which argues against the use of isotope residuals in Mediterranean paleosalinity reconstructions.

1. Introduction

The only widely applied technique for paleo-sea surface salinity (paleo-SSS) determination uses differences between past and present values in $\delta^{18}O$ records from planktonic foraminiferal carbonate. Corrections for changes in sea surface temperature (SST) and for the glacial $\delta^{18}O$ enrichment due to ^{16}O sequestration in continental ice sheets leave a "residual" isotopic difference. This is then translated into salinity change using modern local salinity:$\delta^{18}O$ (S:$\delta^{18}O$) relationships [e.g., *Duplessy et al.*, 1991; *Maslin et al.*, 1995; *Wang et al.*, 1995; *Hemleben et al.*, 1996; *Kallel et al.*, 1997a, b]. However, *Rohling and Bigg* [1998] argued that temporal invariability in any local S:$\delta^{18}O$ relationship would seem unlikely, and *Schmidt* [1998] found that temporal and spatial S:$\delta^{18}O$ gradients are not generally related. For any given basin, therefore, temporal covariations between salinity and $\delta^{18}O$ should be independently assessed. Until alternative analytical paleo-SSS techniques become accepted, such assessments are best made using models that simultaneously solve for salinity and $\delta^{18}O$.

The Mediterranean is ideally suited for such a study, because it is an intensively studied, geographically limited basin with substantial freshwater "sink" and "source" terms and a well-constrained exchange with the open ocean. Resolution of the paleo-SSS problem is particularly relevant in the Mediterranean, since properly quantified Mediterranean paleo-SSS maps would greatly improve our understanding of circulation patterns during the episodic formation of organic carbon enriched sediments (sapropels; see review by *Rohling* [1994]). This includes the definition of restoring boundary conditions for numerical circulation models [*Myers et al.*, 1998]. Finally, definition of volume fluxes and properties of exchange between the Mediterranean and Atlantic will facilitate modeling of ocean-wide oxygen isotope advection from deep-water source areas [*Rohling and Bigg*, 1998; *Schmidt*, 1998].

Paper number 1999PA900042.
0883-8305/99/1999PA900042$12.00

2. Objectives and Strategy

Here, I will (1) simultaneously resolve basin-average salinity and $\delta^{18}O$ changes in the Mediterranean since the Last Glacial Maximum; (2) investigate the different response amplitudes for salinity and $\delta^{18}O$ to changes in freshwater budget and exchange through the Strait of Gibraltar; (3) evaluate whether $\delta^{18}O$ residuals may be used to approximate paleosalinity in the basin through simple temporally invariable S:$\delta^{18}O$ conversion; (4) assess major potential causes for strong $\delta^{18}O$ depletions in Mediterranean sapropels; and (5) approximate volume and property fluxes through time from the Mediterranean into the Atlantic.

To address these problems, a box model is presented that determines hydraulically controlled changes in the exchange transport through the Strait of Gibraltar, in response to global sea level variations and realistically constrained changes in the Mediterranean freshwater budget. To validate the model, simulations of modern rates and properties of exchange transport are compared with observed values, and simulated changes in exchange transport rate over time are compared with a reconstruction based on proxy data from the Alboran Sea. Next, the model simultaneously determines long-term average Mediterranean salinity (S_M) and $\delta^{18}O$ (δ_M) and the isotopic composition of evaporation (δ_E). Simultaneous solving for δ_M and S_M allows direct comparison of temporal changes in these two parameters as caused by the same environmental forcing. Sensitivity tests evaluate the robustness of the simulations with respect to the various assumptions and uncertainties (Table 1). Finally, the model converts δ_M changes into equilibrium calcite values ($\delta_{calcite}$) for comparison with a stacked Mediterranean record based on planktonic foraminifera from five cores (Table 2).

3. Model Description

Complexity of the model and input parameters is reduced to a minimum to emphasize major causes of variability rather than details (Figure 1). Variations in Atlantic inflow are derived from a hydraulic control model for the Strait of Gibraltar. Within the Mediterranean, Atlantic inflow is modified by the various terms in the freshwater budget. The resultant properties define the reported "Mediterranean average values" that characterize outflow into the Atlantic. Conservation of mass and salt is maintained through subsurface outflow from the Mediterranean into the Atlantic. I

Table 1. Parameters Used in the Main Model Run and the Presented Sensitivity Tests

Parameter	Main Run	Sensitivity Test 1 (Figure 6a)	Sensitivity Test 2 (Figure 6a)	Sensitvity Test 3 (Figure 6a)	Sensitvity Test 4 (Figure 6b)	Sensitvity Test 5 (Figure 6b)
V	7.5 m s^{-1}	--	--	--	8.5 m s^{-1}	--
ΔT	see Figure 2	--	--	--	--	0.5°C
r	0.60; 0.65; 0.70; 0.75; 0.80	0.7	0.7	0.7	0.7	0.7
δ_B	see Figure 2	-9‰	--	-9‰	--	--
δ_R	see Figure 2	--	-6‰	-6‰	--	--

Dashes (--) indicate that parameters are treated as in the main model run.

assume unlimited inflow capacity from the Atlantic and outflow capacity into the Atlantic, with these two Atlantic "reservoirs" being separate and unconnected.

Bryden and Kinder [1991] demonstrated that inflow volume from the Atlantic Ocean into the Mediterranean (Q_A) depends on the geometry of the Strait of Gibraltar and on the Mediterranean excess of evaporation over total freshwater input (X). Strait geometry is modified by eustatic sea level change [*Fairbanks*, 1989, 1990]. Using that model, and including variable sea level, *Rohling and Bryden* [1994] defined $Q_A = \Phi\,\Omega\,Q_A^P$, where p stands for present-day and $Q_A^P \approx 23 \times 10^{13}$ m^3 yr^{-1} [*Bryden et al.*, 1994]. The dimensionless parameter Φ (= 1.0 at present) was found to be reduced by 4.3×10^{-3} per meter sea level lowering, while Ω was related to $\gamma = X/X^P$. Initially, $\gamma \approx \Omega^2$ was used [*Rohling and Bryden*, 1994; *Rohling*, 1994]. Improved models, however, indicate that $\gamma \approx \Omega^3$ is more accurate (S. Matthiesen and K. Haines, personal communication, Edinburgh, Sept. 1997), which is therefore used here.

Changes in salinity of Atlantic inflow are considered purely as a function of the glacial concentration effect. This "glacial effect" on salinity (S_{geff}) is determined from the sea level record [*Fairbanks*, 1989, 1990] according to $S_{geff} = (34.74\ z_{sl})\ (3900 - z_{sl})^{-1}$, where z_{sl} stands for sea level lowering in meters, 34.74 is the mean world ocean salinity, and 3900 m is the world ocean average depth [*Maslin et al.*, 1995]. Hence the salinity of Atlantic inflow is determined as $S_A = 36.2 + S_{geff}$, where 36.2 is the modern value [*Bryden et al.*, 1994].

The oxygen isotope composition of Atlantic inflow (δ_A) is also determined as a function of a glacial concentration effect, amounting to 0.012 ± 0.001‰ enrichment per meter sea level lowering [*Labeyrie et al.*, 1987; *Shackleton*, 1987; *Fairbanks*, 1989]. Today, δ_A is about 1.0‰ [*Pierre*, 1999], so that $\delta_A = 1.0 + 0.012\ z_{sl}$. Recently, *Schrag et al.* [1996] suggested that a more accurate value for the glacial enrichment would be only 0.008‰ m^{-1}. If true, the model results overestimate glacial isotopic enrichment by a maximum of 0.3‰. This does not affect the main conclusions.

Mediterranean evaporation rate E is calculated with the latent heat flux equation $Q_L = \rho_a\ L\ C\ V\ [q_{sat(SST)} - r\ q_{sat(Ta)}]$, where ρ_a is density of air (1.2 kg m^{-3}), L is latent heat of vaporization equal to about 2.5×10^6 J kg^{-1}, and C is the exchange coefficient of 1.15×10^{-3} [*Garrett et al.*, 1993; *Wells*, 1995]. Wind speed V is treated as a constant at 7.5 m s^{-1}, the average value observed between 1945 and 1990 [*Garrett et al.*, 1993]. Parameter $q_{sat(SST)}$ is the saturation mixing ratio at sea surface temperature (SST), $q_{sat(Ta)}$ is the saturation mixing ratio at the temperature Ta measured at 10 m above the sea surface, and r is the relative humidity (sea-air temperature difference ΔT = SST - Ta) [*Abbott and Tabony*, 1985; *Wells*, 1986; *Wells and King-Hele*, 1990]. Parameter q_{sat} is calculated from the vapor pressure e_{sat}, according to $q_{sat} = (m_v/m_d)\ e_{sat}\ (p - e_{sat})^{-1}$, where p is total pressure at mean sea level (1.012×10^5 Pa), m_v/m_d is the ratio between molecular weights of water vapor and dry air, and $e_{sat} = 10^2 \exp\{55.17 - 6803\ (T+273.15)^{-1} - 5.07 \ln(T+273.15)\}$ as expressed in Pa [*Abbott and Tabony*, 1985;

Table 2. Details of the Cores Used in the Stacked Mediterranean $\delta^{18}O$ Record

Core	Latitude	Longitude	Depth, m	Species	Average Resolution[a], years	Core-Top $\delta^{18}O$[b], ‰	Reference
MD84-641	33.02°N	32.38°E	1375	*G. ruber*	600	0.84	*Fontugne and Calvert* [1992]
IN68-9	41.47° N	17.54°E	1234	*G. bulloides*	300	1.12	*Rohling et al.* [1997]
T26B	34.44°N	16.48°E	2415	*G. ruber*	400	-0.30	*Troelstra et al.* [1991]
BC15	41.57°N	05.56°E	2500	*N. pachyderma*	700		*Rohling et al.* [1998]
KS8230	36.27°N	03.53°W	795	*G. bulloides*	550	0.65	*Pujol and Vergnaud-Grazzini* [1989]

[a] Average resolution concerns the original data through the relevant interval of the last 20 kyr.
[b] Where core-top corresponds roughly to 0 ka B.P.

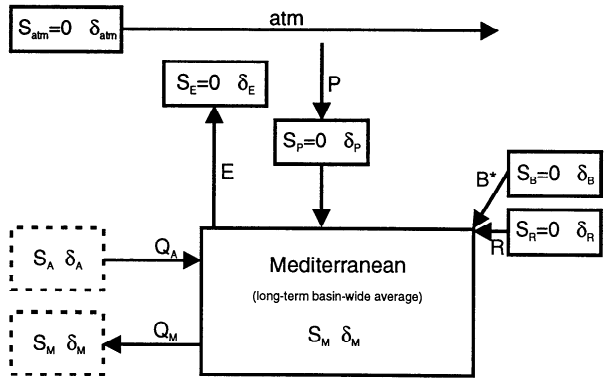

Figure 1. Layout of the model used to determine long-term basin-wide average Mediterranean salinity and $\delta^{18}O$. Atlantic boxes are indicated with broken lines to imply unlimited capacity of these two reservoirs that are taken to be unconnected.

Wells, 1986]. Using SST for T gives $e_{sat(SST)}$ and $q_{sat(SST)}$, while use of Ta gives $e_{sat(Ta)}$ and $q_{sat(Ta)}$. Latent heat flux Q_L is found in W m^{-2}, and to determine E, this is converted according to 1 W ≡ 1.26 cm yr^{-1} per unit area [*Wells*, 1986; *Garrett et al.*, 1993].

Today, Mediterranean annual average SST is about 19 °C [*Stanev et al.*, 1989]. Glacial average SST is taken to be about 5°C lower [*Bigg*, 1994, 1995], and the temperature change is split equally over the two deglaciation intervals (Figure 2). Note that the glacial temperatures of *Bigg* [1994; 1995] were not obtained from oxygen isotope data. The present-day annual average sea-air temperature difference (ΔT) is hard to estimate on a basin-wide scale, but a typical value of 0.5°C [*Gorshkov*, 1978; *Naval Oceanography Command Detachment*, 1981] with $0.70 < r < 0.75$ gives a modern value for $q_{sat(SST)} - r\, q_{sat(Ta)}$ around 4×10^{-3}, a fair approximation of the 1945-1990 average value of 3.7×10^{-3} [*Garrett et al.*, 1993]. Past ΔT is varied in a simple linear fashion in accordance with the SST changes to account for colder airflow over the enclosed Mediterranean Sea during glacial times with enhanced land-sea temperature contrasts [*Bigg*, 1994, 1995] (Figure 2). The glacial value for ΔT is set at 1.5°C, a typical modern wintertime value [*Gorshkov*, 1978; *Naval Oceanography Command Detachment*, 1981]. As the imposed temporal variation in ΔT is a first-order assumption, a sensitivity test is performed using a constant value of 0.5°C (Table 1).

Precipitation over sea (P) is varied with E, maintaining the present-day proportional relationship $P \approx 0.4\ E$ [*Garrett et al.*, 1993]. Constant proportionality is assumed, because the amount of rain-out over sea is more or less a function of (1) the general geographic setting, which has not changed since the Last Glacial Maximum, and (2) the large-scale atmospheric circulation patterns where midlatitude westerlies interact with subtropical high-pressure influences, the organization of which was roughly similar to the present [*Kutzbach et al.*, 1993].

Runoff values R are schematically specified in the form of a ratio relative to the present (Figure 2). Runoff is taken to be similar to the present at about 0.45×10^{12} m^3 yr^{-1} [*Garrett et al.*, 1993], except for the early Holocene period, during which the formation of sapropel S1 was at its peak, when runoff was strongly increased [cf. *Street and Grove*, 1979; *Adamson et al.* 1980; *Rossignol-Strick et al.*, 1982; *Béthoux*, 1984; *Shaw and Evans*, 1984; *Rossignol-Strick*, 1987; *Klein et al.*, 1990; *Wijmstra et al.*, 1990; *Rohling and Hilgen*, 1991; *Rohling*, 1994]. Following the overall indications from those authors, doubled runoff values are used for this period, with linear increases and decreases on either side of the peak over 2.5 kyr intervals (Figure 2), so that the total period of increased R covers the 5 to 6 kyr since the last precession minimum spanning the buildup and decay of specific conditions associated with sapropel formation [*Hilgen*, 1991; *Rohling*, 1994; *Higgs et al.*, 1994; *Aksu et al.*, 1995; *Thomson et al.*, 1995; *Rohling et al.*, 1997; *Reichart et al.*, 1998].

Variations in relative Black Sea input B are after a recent model for the deglacial history of exchange transport between the Black Sea and the Mediterranean [*Lane-Serff et al.*, 1997] (Figure 2), with a modern (before damming) freshwater drainage through that basin of 0.20×10^{12} m^3 yr^{-1} [*Tolmazin*, 1985; *Oguz et al.*, 1990; *Lane-Serff et al.*, 1997]. Although of lower temporal resolution than the model of *Arthur and Dean* [1998], the *Lane-Serff et al.* [1997] model does account for a 1000 year lag of Black Sea outflow after the reconnection with the Mediterranean by sea level rise. A third model [*Ryan et al.*, 1997] advocates that outflow started yet another

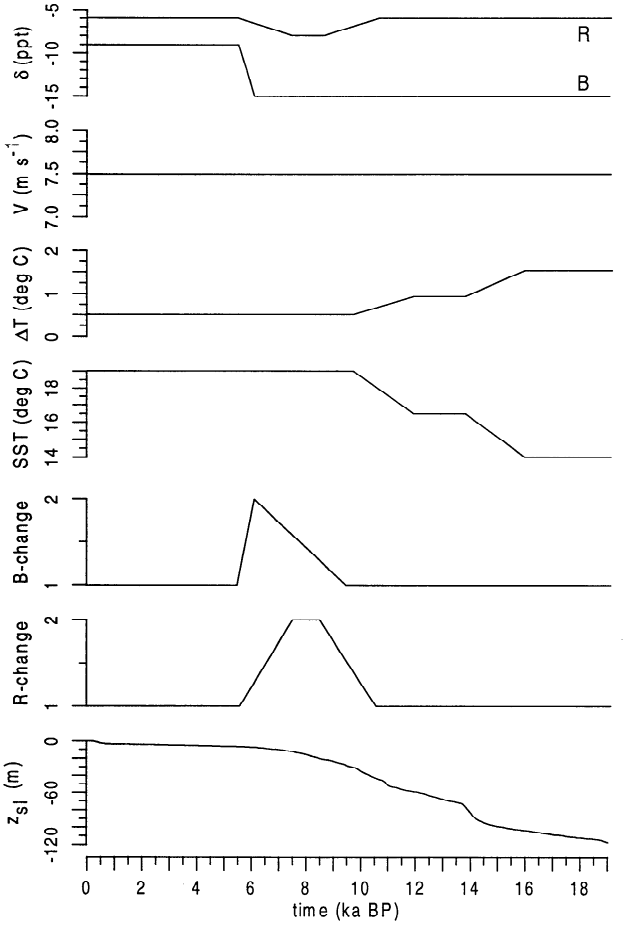

Figure 2. Changes with time in the input functions as used in the main experiment. Shapes of the curves are as discussed in the text. Scenarios are calculated for different values of relative humidity r. Sensitivity experiments assess the assumptions of constant wind speed, and of the displayed sea-air temperature contrast (ΔT = SST−Ta) and oxygen isotopic compositions for Black Sea outflow B and runoff R. Changes in volumes of Black Sea outflow (B change) and runoff (R change) relative to the present and changes in sea surface temperature (SST) are as discussed in the text. Changes in sea level are after *Fairbanks* [1989, 1990].

1000 years later, because of later (tectonic) reconnection of the two basins. Here, the *Lane-Serff et al.* [1997] reconstruction is used because it presents the intermediate scenario for timing of the Black Sea reconnection. The present study demonstrates that, for the Mediterranean as a whole, variations in Black Sea outflow played an inferior role to changes in overall runoff. Black Sea properties are taken to be the net throughput through that basin so that they actually relate to the excess drainage into the Black Sea, compounded by the enhanced freshwater outflux upon reconnection as modeled by *Lane-Serff et al.* [1997].

Combined, E, P, R, and B determine the Mediterranean excess of evaporation over total freshwater input X according to $X = E - P - R - B$. The calculated modern values for X with $0.70 < r < 0.75$ range between 0.47 and 0.60 m yr^{-1}, in agreement with recently determined values of 0.52 [*Bryden et al.*, 1994] and 0.56-0.66 m yr^{-1} [*Garrett et al.*, 1993]. Salinity S for each of the freshwater budget terms is zero. Absence of external sources and sinks for salt defines S as a conservative property, constrained by conservation of mass and salt. Consequently, the general average salinity in the Mediterranean S_M is given by $S_M = Q_A S_A (Q_A - X)^{-1}$. Regarding isotopic compositions, the situation is different in that values for the various freshwater budget terms are different from one another and also have varied through time.

During evaporation, equilibrium fractionation between vapor and surface water depends on SST as described by *Majoube* [1971]: $\alpha_{evap} = \exp\{1.137\ (SST+273.15)^{-2} \times 10^3 - 0.4156\ (SST+273.15)^{-1} - 2.0667 \times 10^{-3}\}$. The isotopic composition of evaporating water is then determined after *Craig and Gordon* [1965] and *Gonfiantini* [1986], using the ratio between total evaporation rate (E) and that for the isotopic species (E_i). Rewriting the equations to fully account for ΔT in the vapor pressure terms gives

$$\delta_E = \frac{\frac{(1+\delta_M)}{\alpha_{evap}} - \frac{q_{sat(Ta)}}{q_{sat(SST)}}\, r\, (1+\delta_{atm})}{(1 - \frac{q_{sat(Ta)}}{q_{sat(SST)}}\, r)\, \frac{\rho_i}{\rho}} - 1$$

In this equation, the δ values should be used fully expressed as value $\times 10^{-3}$. The ρ values are resistance coefficients (not to be confused with density). *Gonfiantini* [1986] concluded that a realistic value for ρ_i/ρ in natural circumstances is 1.0142, but lower values were implied by *Merlivat and Jouzel* [1979] and *Gat* [1996]. As discussed, the present model produces realistic modern values for $q_{sat(SST)} - r\, q_{sat(Ta)}$ and consequently for X and S_M, when $r \approx 0.70$. For that value, $\rho_i/\rho = 1.0142$ gives more realistic isotopic results than lower values and hence is used here. Parameter δ_M is the isotopic composition of Mediterranean waters (the model does not differentiate surface from deep waters (Figure 1)), and δ_{atm} is the isotopic composition of atmospheric vapor outside the boundary layer, which is kept in equilibrium with δ_P, while $\delta_P = \delta_R$. Significance of these choices for δ_{atm} and δ_P is discussed below.

Values for δ_B and δ_R are specified input parameters (Table 1, Figure 2). In the main experiment, the value for δ_B since establishment of the modern circulation pattern [*Lane-Serff et al.*, 1997] is taken to be equal to the modern average value of freshwater drainage into the Black Sea, which is about -9‰ [*Swart*, 1991]. Late glacial values and those of the fresh water expelled upon reconnection [*Lane-Serff et al.*, 1997] are specified to reflect a glacial origin, using a modern North Siberian value of -15‰ [*Rozanski et al.*, 1993]. Transition between the two values is linear over 1 kyr, the typical timescale for flushing of glacial fresh water out of the Black Sea [*Lane-Serff et al.*, 1997]. The basin average for δ_R in the main experiment is -6‰, with an extra 2‰ depletion in the interval with double runoff bound by similar linear changes to those in R (Figure 2). The 2‰ extra depletion is based on $\delta^{18}O$ studies of snail shells from the Negev desert [*Goodfriend*, 1991] and of speleothems in Soreq cave (Israel) [*Bar-Matthews et al.*, 1997, 1999], corroborated by even greater depletions in fossil North African waters [*Sonntag et al.*, 1979; *Sultan et al.*, 1997] and in lacustrine carbonates deposited in Nile headwaters at times of sapropel deposition [*McKenzie*, 1993]. Extra depletion during wet episodes is likely due to the so-called amount effect [*Bar-Matthews et al.*, 1997, 1999], which causes about 1.5‰ extra depletion for every 100 mm increase in precipitation in (sub)tropical stations [cf. *Rozanski et al.*, 1993; *Joussaume and Jouzel*, 1993; *Hoffman and Heimann*, 1997]. The sensitivity experiments (Table 1) evaluate the importance of the defined values for δ_B and δ_R and also of mean wind speed V.

Since δ_E and δ_M are interrelated, they are determined iteratively, with $\delta_M = (Q_A \delta_A + R \delta_R + B \delta_B + P \delta_P - E \delta_E)(Q_A - X)^{-1}$. Although typically fewer than 15 iterations were needed, each experiment was iterated over 20 steps. In the main experiment, δ_{atm} is kept in equilibrium with δ_P, while $\delta_P = \delta_R$. To evaluate his choice, a separate experiment started iteration with those relationships but then allowed variation according to $\delta_{atm} = \delta_E + 1000\ (\alpha_{cond} - 1)\ \ln(f)$ [*Rozanski et al.*, 1982]. Here f is the fraction of vapor remaining after rain-out (≈ 0.6 for $P \approx 0.4\ E$), and α_{cond} is the equilibrium fractionation factor after *Majoube* [1971] at condensation temperature (using SST-5°C). Values for δ_P then were determined in equilibrium with atmospheric vapor, averaging the change in δ_{atm} associated with change in f from 1.0 to 0.6. This test returned up to 0.3‰ higher values for δ_M than the main experiment, throughout the simulated record. General trends remain similar to those in the main experiment, to within 6% accuracy. Hence the choice of relationship between δ_{atm} and δ_P does not substantially affect the conclusions drawn in this paper.

Using δ_M, the average Mediterranean $\delta^{18}O$ record for calcite formed in surface water at equilibrium ($\delta_{calcite}$) is determined using the *O'Neil et al.* [1969] relationship $\alpha_{calc} = \exp\{2.78\ (SST+273.15)^{-2} \times 10^3 - 3.39 \times 10^{-3}\}$ within $\delta_{calcite} = 10^3 \ln(\alpha_{calc}) + (\delta_M - 30.92)\ 1.03092^{-1}$, which is corrected for the difference between values versus Standard Mean Ocean Water (SMOW) for water and versus Pee Dee Belemnite (PDB) for calcite [*Coplen et al.*, 1983; *National Institute of Standards and Technology*, 1992].

Simulated $\delta_{calcite}$ records are compared with a mean Mediterranean planktonic foraminifera-based $\delta^{18}O$ record, obtained from stacking five records from sites spread throughout the Mediterranean (Alboran Sea, Gulf of Lions, Ionian Sea, Adriatic Sea, and southern Levantine basin) (Table 2). Both the geographic spread and the fact that these data are based on different planktonic foraminiferal species (living at different depths and seasons) are relevant to the creation of an "average Mediterranean" stack for comparison with the simulated record. For stacking, the observational records are normalized to their average core-top value (0.58‰, Table 2). One record lacks most of the Holocene and is therefore normalized to the model-produced isotopic value at the age of the core top. Next, the records are linearly interpolated and read out at 100 year intervals to calculate means and $\pm 1\sigma$ intervals (Figure 3a). The stack serves for comparison only and does not function as input into the calculations.

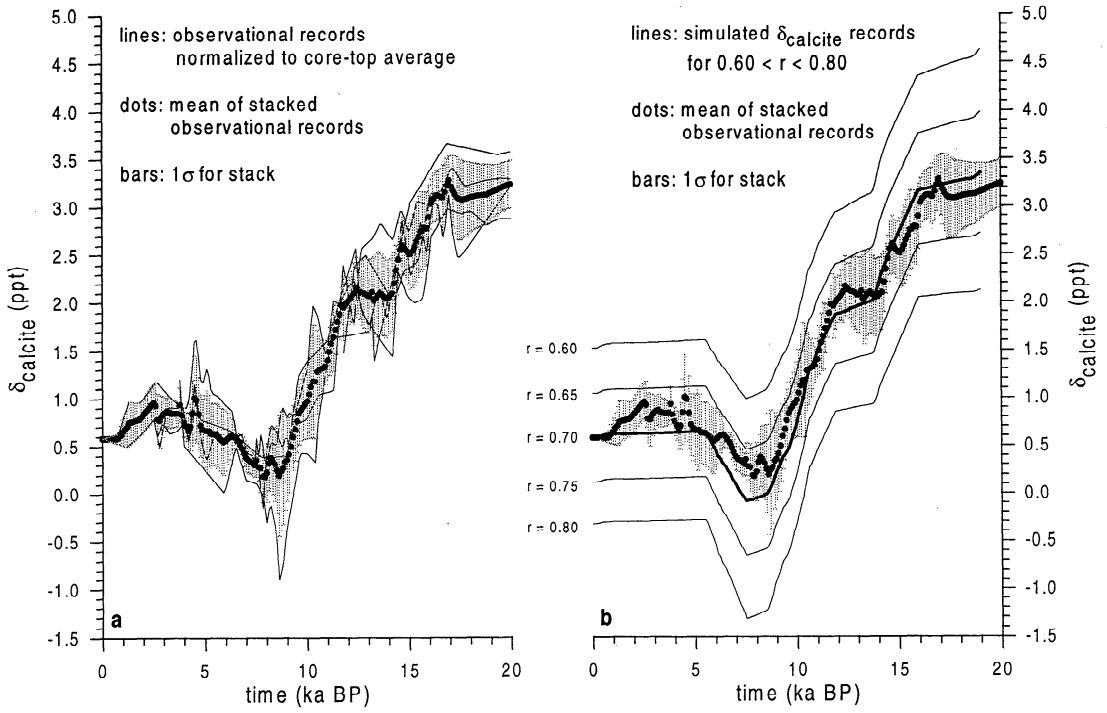

Figure 3. (a) Stack of five Mediterranean oxygen isotope records versus time (see Table 2), with mean values (dots) and ±1σ interval (bars); (b) comparison of stacked record with simulated $\delta_{calcite}$ records for $0.60 < r < 0.80$.

4. Discussion

4.1. Model Results, Sensitivity Experiments, and Implications

The simulations of relative inflow volume from the Atlantic show three main episodes of increase, starting around 14-14.5 ka B.P., 11 ka B.P., and 7-8 ka B.P. (Figure 4). *Rohling et al.* [1995] ascribed development of dominance of *Globorotalia inflata* around 8 ka B.P. in the Alboran Sea to onset of permanent frontal systems associated with the main gyres in that basin, due to sufficiently increased inflow volume. All simulated increases in the rate of inflow are contemporaneous with abundance increases of *G. inflata* in Alboran Sea core KS310 within the limits of the chronostratigraphic resolution (Figure 4). This suggests that the model reasonably approximates changes in the basin's mass balance over the past 20,000 years, which supports its use for evaluation of changes in basin-average salinity and $\delta^{18}O$ (S_M and δ_M, respectively).

The greatest influence on modeled S_M and δ_M is exerted by r (Figure 5). For $r = 0.70$, $S_M \approx 38.7$, giving an outflow-inflow salinity contrast of around 2.5, only a few tenths higher than observed [*Bryden and Kinder*, 1991; *Bryden et al.*, 1994; *Pierre*, 1999]. The oxygen isotope contrast between outflow and inflow for $r = 0.70$ is 0.43‰, in agreement with observational values between 0.4 and 0.5‰ [*Pierre*, 1999]. The ratio $(\delta_M-\delta_A)/(S_M-S_A)$ equals 0.17 for $r = 0.70$ and 0.14 for $r = 0.75$. The average Mediterranean value for this ratio in the western Alboran Sea is around 0.20 [*Pierre*, 1999]. Using $r = 0.70$, the simulated present-day $\delta_{calcite}$ value is 0.58‰. The average value for the tops of the stacked cores is 0.58‰ (Table 2), while a larger suite of 64 core-top values gives a mean of 0.67 plus or minus a 1σ interval of 0.68‰ (Table 3). Because of these good agreements with observations, the reconstruction for $r = 0.70$ is used as a standard against which sensitivities to the main assumptions are evaluated.

Sensitivity experiments 1, 2, and 3 (Table 1; Figure 6a) indicate that the general shape of the simulated δ_M record hardly depends on variability of δ_B. In contrast, the relatively small variability allowed in δ_R between about 10 and 5 ka B.P. does importantly determine the depletion in δ_M at that time. This depletion virtually disappears when δ_R is kept constant at its present-day value, despite the fact that even that scenario contains temporarily doubled runoff volumes (Figure 2).

Sensitivity to changes in mean wind speed is relatively small for δ_M (experiment 4, Table 1; Figure 6b). This might be different should a "jump" be made from a rough regime ($V > 7$ m s^{-1}) to a smooth regime ($V < 7$ m s^{-1}) [*Merlivat and Jouzel*, 1979]. The present-day Mediterranean, however, ranges in the rough regime ($V \approx 7.5$ m s^{-1} [*Garrett et al.*, 1993]), and glacial mean wind speeds are more likely to have been similar or higher than today, rather than lower [*Dong and Valdes*, 1995; *Myers et al.*, 1998]. The S_M record is somewhat more sensitive to changes in V (Figure 6c). However, since detailed wind-speed information is hard to obtain from geological data, a constant value of 7.5 m s^{-1} is used.

The defined variability in the sea-air temperature contrast (ΔT) (Figure 2) is evaluated in experiment 5 (Table 1; Figures 6b and 6c). Variable ΔT yields δ_M and S_M values that are up to 0.5‰ and 0.6 higher, respectively, than those found for constant $\Delta T = 0.5$°C. Although significant, these differences fall within the effects of a less than 3% variability of the relative humidity term r on δ_M and S_M (Figure 5). The uncertainty in the determination of ΔT could therefore be viewed as the equivalent of an error in r of up to 3%, so that r for the standard reconstruction ranges between apparent values of 0.70 (ΔT variable as in Figure 2) and 0.67 (ΔT constant at 0.5°C).

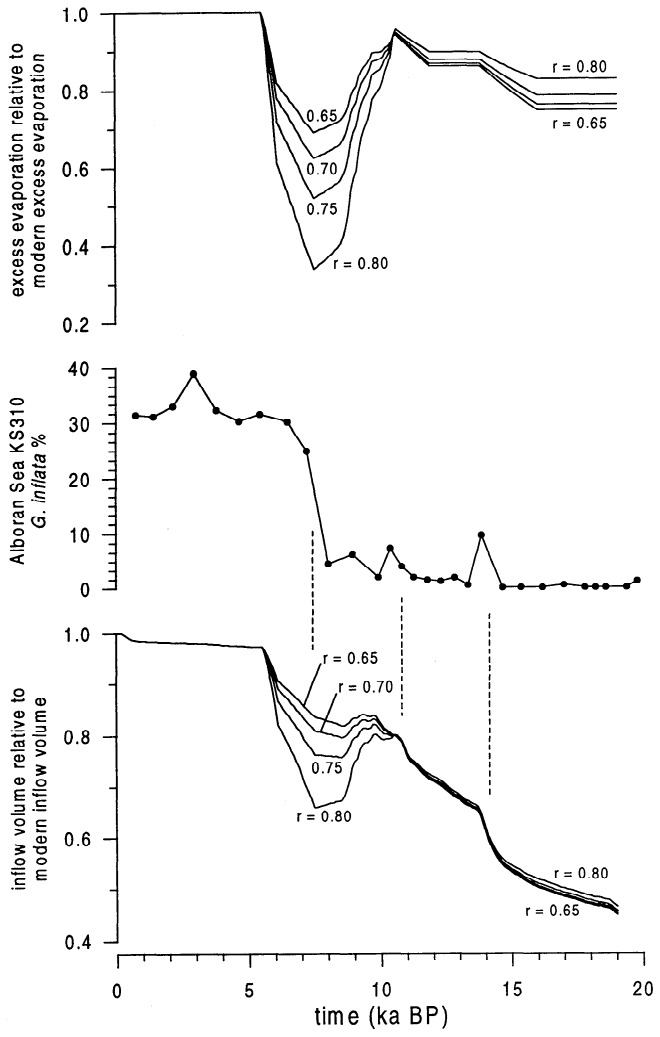

Figure 4. Simulated changes in inflow volumes through the Strait of Gibraltar, and in Mediterranean excess evaporation over freshwater input, for various values of relative humidity r, in comparison with relative abundance variations of *Globorotalia inflata* in core KS310 from the Alboran Sea [*Rohling et al.*, 1995].

Equilibrium calcite ($\delta_{calcite}$) records for the various values of r (Figure 3b) are naturally very similar to the δ_M records (Figure 5), with an overprint of the applied SST variations (Figure 2), and are directly compared with the stacked observational record (Figure 3). In view of the above discussion of the equivalent effect of uncertainty in ΔT, it is important that the $\delta_{calcite}$ simulations for $0.67 < r < 0.70$ encompass virtually the entire stacked record (Figure 3b), which implies that the model realistically simulates absolute values, trends, and response magnitudes in $\delta_{calcite}$ and therefore δ_M. This strongly supports application of the model's interrelated set of calculations for simultaneous assessment of S_M and δ_M responses to changes in the freshwater cycle and in exchange transport through the Strait of Gibraltar. The close match between the stacked and simulated $\delta_{calcite}$ records (Figure 3b) also suggests that relative humidity over the Mediterranean Sea was more or less constant (around $r = 0.70$) throughout the past 20,000 years. *Rozanski* [1985] reached a similar conclusion for the North Atlantic. For an open oceanic setting, this is not unexpected, since *Gorshkov* [1978] shows that present-day relative humidity values are fairly uniform over the entire world ocean, regardless of climatic zones. The temporal constancy of relative humidity over the Mediterranean inferred here is more surprising, since the basin is tightly enclosed by land masses that experienced major hydrological changes [*Sonntag et al.*, 1979; *Adamson et al.*, 1980; *Rossignol-Strick et al.*, 1982; *Rossignol-Strick*, 1987; *Guiot et al.*, 1989; *Klein et al.*, 1990; *Wijmstra et al.*, 1990; *Goodfriend*, 1991; *Rohling and Hilgen*, 1991; *Sultan et al.*, 1997; *Reichart et al.*, 1998].

The model shows less dramatic temporal variability in the Mediterranean-Atlantic salinity contrast ($\Delta S_{M\text{-}A}$) than in the $\delta^{18}O$ contrast ($\Delta\delta_{M\text{-}A}$) (Figure 5). For $r = 0.70$, the $\Delta\delta_{M\text{-}A}$ record suggests a reversal of the gradient from +0.4‰ today to −0.5‰ around 8 ka B.P., while $\Delta S_{M\text{-}A}$ was not at all reversed, but only somewhat weakened relative to the present. Hence a flat or reversed Atlantic-Mediterranean isotope gradient, as inferred for times of the early Holocene sapropel S1 formation [*Thunell and Williams*, 1989; *Kallel et al.*, 1997a], would have occurred while the salinity gradient remained at about 80% of its present value. Consequently, there would have been substantial buoyancy loss and related antiestuarine overturn in the basin, albeit weakened relative to the present. The numerical circulation model of *Myers et al.* [1998] predicts active antiestuarine circulation above 400 m and dramatic cessation of ventilation below that depth in the eastern Mediterranean in response to a moderate reduction in the surface water salinity gradient. Deep water stagnation then allowed development of bottom water anoxia and sapropel deposition. The reduced salinity gradient would have partly resulted from enhanced runoff (Figure 2), which is thought to be related to the inferred extra δ_R depletion via the amount effect (section 3).

An interesting speculation concerns the nature of stronger δ_M depletions, such as that in sapropel S5 of the penultimate interglacial maximum [eg., *Cita et al.*, 1977; *Vergnaud-Grazzini et al.*, 1977; *Vergnaud-Grazzini*, 1985; *Rohling et al.*, 1993]. At first sight, these would be interpreted in terms of greater freshwater input into the Mediterranean, or stronger isotopic depletion in the major freshwater sources, compared to the Holocene. However, a potential third alternative now emerges, namely, that the penultimate interglacial maximum was characterized by slightly higher relative humidity values than the Holocene. Coupled ocean-atmosphere circulation models are needed that realistically solve for changes in vegetation and evapotranspiration to assess whether this is a realistic option, accounting for the several degrees Celcius higher global temperatures of that time [*CLIMAP*, 1984; *Jouzel et al.*, 1987; *Guiot et al.*, 1989], which would have favored higher atmospheric vapor loads (specific humidity).

Nonproportionality between responses of $\Delta\delta_{M\text{-}A}$ and $\Delta S_{M\text{-}A}$ (Figure 5) limits the use of oxygen isotope residuals to reconstruct paleosalinity. Time-slice maps of isotope residuals remain a valid means to trace lateral trends and should by preference be used in their own right. Further interpretation in terms of salinity change or freshwater gain/loss is not a trivial problem, which centers around determination of an appropriate spatial S:$\delta^{18}O$ gradient for the specific period of investigation. Use of temporal gradients to calibrate spatial gradients is not straightforward (Figure 5c), as was also demonstrated by *Schmidt* [1998].

4.2. Evaluation of Negative δ_M

Here, I analyze the counterintuitive result of a negative net isotopic effect at certain times with considerable excess evaporation over freshwater input X, so that the Mediterranean shows oxygen isotope depletion relative to the Atlantic, whereas salinity increases in the basin in a similar fashion to today. This may be visualized by considering the export of depleted freshwater ($E\delta_E$) versus the

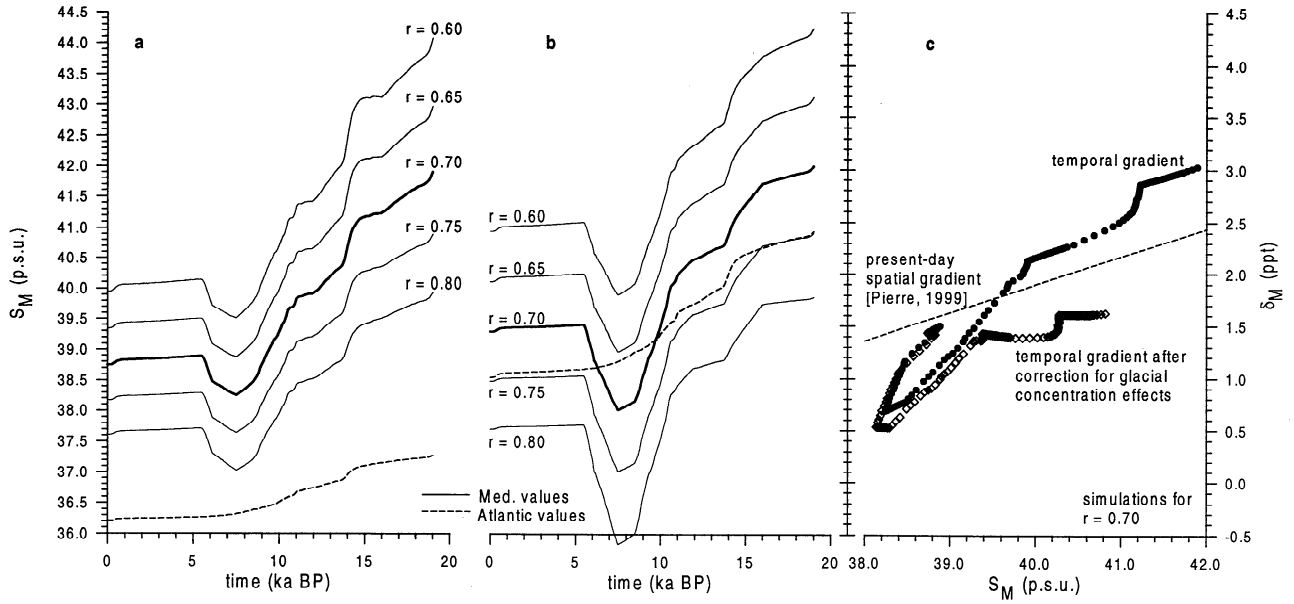

Figure 5. (a) Simulated record versus time for Mediterranean seawater salinity, for various values of relative humidity r (solid lines). Simulated changes in salinity of Atlantic inflow are also indicated (dashed lines). (b) Same as for Figure 5a but for $\delta^{18}O$. (c) S_M:δ_M plot, for comparison of the present-day spatial S:$\delta^{18}O$ gradient [*Pierre*, 1999] with the simulated temporal gradient (solid dots) and the simulated temporal gradient after correction for glacial enrichments (open diamonds) (simulations for $r = 0.70$).

Table 3. Mediterranean Core-Top $\delta^{18}O$ Values for Various Planktonic Foraminiferal Species

Core	Species	Core-Top $\delta^{18}O$	Latitude	Longitude
KC82-41	*bulloides*	0.04	36.00°N	04.24°W
KS82-30	*bulloides*	0.65	36.27°N	03.53°W
KS82-30	*ruber*	0.07	36.27°N	03.53°W
SU81-07	*bulloides*	0.81	35.57°N	03.48°W
KS82-31	*bulloides*	0.24	36.09°N	03.17°W
KS82-31	*ruber*	0.27	36.09°N	03.17°W
KS82-32	*bulloides*	0.37	36.07°N	02.07°W
KS70-06	*ruber*	0.5	38.31°N	04.00°E
KS70-06	*bulloides*	1.5	38.31°N	04.00°E
KS70-06	*inflata*	1.6	38.31°N	04.00°E
1960,201	*ruber*	-0.3	37.21°N	04.51°E
1960,201	*inflata*	1.6	37.21°N	04.51°E
KET80-22	*bulloides*	1.58	40.35°N	11.43°E
KET80-19	*bulloides*	1.54	40.33°N	13.21°E
KET80-19	*ruber*	0.71	40.33°N	13.21°E
KET80-04	*bulloides*	1.67	39.40°N	13.34°E
KET80-03	*bulloides*	1	38.49°N	14.30°E
KET80-03	*bulloides*	1.43	38.49°N	14.30°E
CS72-37	*bulloides*	1.31	36.41°N	12.17°E
CS72-37	*ruber*	0.22	36.41°N	12.17°E
CS70-05	*bulloides*	0.77	35.44°N	13.11°E
T87/26B	*ruber*	-0.25	34.44°N	16.48°E
KET82-22	*ruber*	0.03	37.56°N	16.53°E
MD84-658	*ruber*	0.58	35.02°N	17.38°E
RC9-191	*ruber*	0.59	38.11°N	18.02°E
BAN8409GC	*ruber*	0.7	34.19°N	20.01°E
IN68-9	*bulloides*	1.12	41.48°N	17.55°E
KET82-16	*ruber*	0.79	41.31°N	17.59°E
IN68-5	*bulloides*	1.6	41.14°N	18.32°E
Core 20	*ruber*	0.8	38.26°N	24.58°E
Core 19	*ruber*	0.4	39.16°N	24.50°E
Core 03	*ruber*	0.4	40.08°N	24.51°E
TR171-24	*bulloides*	2.45	34.03°N	22.43°E
T87/2/20G	*ruber*	1.08	34.58°N	23.45°E
MO67-03	*ruber*	1.4	34.25°N	24.50°E
RC9-181	*ruber*	0.1	33.25°N	25.01°E
TR171-27	*bulloides*	1.03	33.50°N	25.59°E
TR171-27	*ruber*	0.41	33.50°N	25.59°E
TR171-27	*universa*	0.26	33.50°N	25.59°E
TR171-27	*aequilat.*	1.31	33.50°N	25.59°E
TR171-27	*ruber*	0.05	33.50°N	25.59°E
TR171-27	*universa*	0.87	33.50°N	25.59°E
TR171-27	*aequilataralis*	1.18	33.50°N	25.59°E
TR171-27	*ruber pink*	-0.63	33.50°N	25.59°E
TR171-27	*sacculifer*	-0.05	33.50°N	25.59°E
KS75-52	*ruber*	0.1	34.00°N	26.19°E
V10-49	*ruber*	0.58	36.05°N	26.50°E
KS75-50	*ruber*	-0.2	34.41°N	27.00°E
KS82-01	*ruber*	0.2	34.22°N	27.09°E
V10-51	*ruber*	0.52	35.55°N	27.18°E
RC9-178	*ruber*	0.12	33.44°N	27.55°E
TR171-22	*bulloides*	1.14	35.19°N	29.01°E
TR171-22	*ruber*	0.54	35.19°N	29.01°E
TR171-22	*inflata*	1.79	35.19°N	29.01°E
TR171-22	*universa*	1.3	35.19°N	29.01°E
TR171-22	*aequilateralis*	1.28	35.19°N	29.01°E
CHN119-16	*ruber*	0.72	33.15°N	30.20°E
P6508-36B	*ruber*	0.49	32.44°N	30.31°E
CHN119-18	*ruber*	0.74	34.21°N	30.56°E
CHN119-22	*ruber*	0.93	32.46°N	31.53°E
MD84-641	*ruber*	0.84	33.02°N	32.38°E
Core 17	*ruber*	-0.75	35.30°N	33.20°E
GA32	*ruber*	-1	31.57°N	34.21°E
Core 190	*ruber*	-0.3	36.00°N	34.23°E

Core-top $\delta^{18}O$ values are corrected after *Rohling and De Rijk* [1999], where a print error made all values negative.

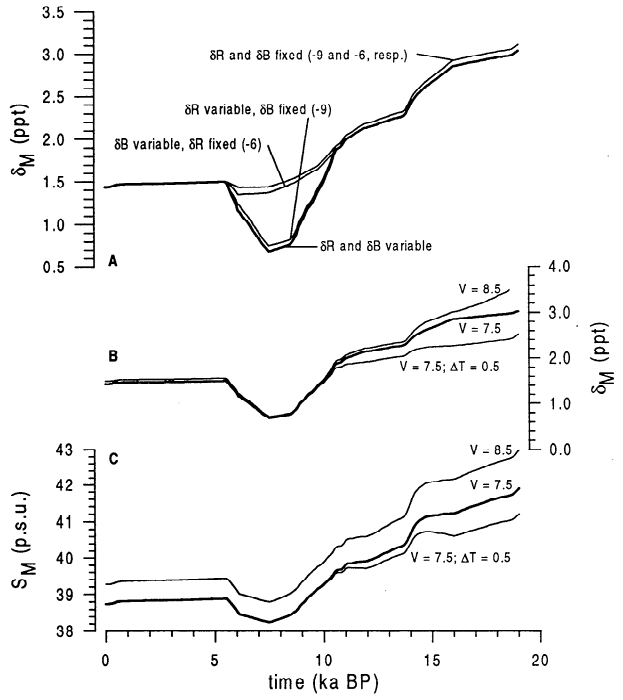

Figure 6. Sensitivity experiments, all using $r = 0.70$: (a) investigation of the relative influences of the imposed variability in δ_R and δ_B; (b) investigation of impact on simulated δ_M of a glacial increase in wind speed to 8.5 m s^{-1}, instead of a constant value of 7.5 m s^{-1} throughout the past 20,000 years, and assessment of the influence of a constant sea-air temperature contrast of 0.5°C, instead of the variable value given in Figure 2; and (c) as in Figure 6b but for Mediterranean salinity.

import of depleted freshwater ($P\delta_P + R\delta_R + B\delta_B = F\delta_F$, where F is the total volume of freshwater inflow and δ_F is the volumetrically weighted average isotope composition of the freshwater input). There would be no net isotopic change when $F\delta_F = E\delta_E$, so that a critical value for δ_E may be defined as $\delta_E^{crit} = F\,E^{-1}\,\delta_F$ or $\delta_E^{crit} = (E\text{-}X)\,E^{-1}\,\delta_F$. The basin would show enrichment (as today) when $\delta_E < \delta_E^{crit}$, whereas overall depletion would occur when $\delta_E > \delta_E^{crit}$.

For the period of S1 deposition, with $r \approx 0.70$, the model gives $(E\text{-}X)E^{-1} \approx 0.7$ (compared with 0.6 today), while the value for δ_F for that period in the main experiment is −8.2‰ (compared with −6.3‰ today), so that $\delta_E^{crit} \approx -6$‰. Therefore the basin could develop isotopic depletion if, at that time, $\delta_E > -6$‰. The equation for δ_E (section 3) shows predominant influences of r and δ_{atm}. Using appropriate values for the period of S1 deposition, $q_{sat(Ta)}/q_{sat(SST)} = 0.97$, $\delta_M \approx 0.75$‰, and $\alpha_{evap} = 1.0099$, the distribution pattern of δ_E as a function of r and δ_{atm} allows identification of the area where, roughly, $\delta_E > -6$‰ (Figure 7). For δ_{atm} in equilibrium with $\delta_P = \delta_R = -8$‰ at that time, the returned value for δ_E is conducive to isotopic depletion in the basin when r is equal or larger than about 0.68. This underlies the model's negative isotopic effect in the runs with $r = 0.70$ and above, while those runs at the same time maintained considerable excess evaporation and thus salinity increase in the basin.

5. Conclusions

A box model representing long-term average conditions in the Mediterranean simultaneously solves for changes in salinity and $\delta^{18}O$. In spite of its basic configuration and schematic input, the model successfully simulates (1) present-day Atlantic-Mediterranean seawater salinity and $\delta^{18}O$ (using relative air humidity of 70%); (2) variations in inflow volume through the Strait of Gibraltar as inferred also from micropaleontological records; and (3) changes in basin-average $\delta^{18}O$ of planktonic foraminiferal calcite since the Last Glacial Maximum. This justifies the use of the model to explore the nature and principal causes of temporal changes in Mediterranean salinity and sea-water $\delta^{18}O$ (S_M and δ_M, respectively).

Volume and property fluxes from the Mediterranean into the Atlantic since the last glacial maximum are assessed with the model and presented graphically for potential use in North Atlantic circulation models (data in centennial time steps are available on request).

Foraminiferal carbonate-based $\delta^{18}O$ records reflect distinct δ_M depletions within sapropels. Such depletions are found to likely indicate that runoff at those times was isotopically more depleted than today. Particularly strong oxygen isotope depletions could indicate slight (of the order of 5%) increases in relative air humidity over the basin, relative to the present. Further studies are needed to evaluate the feasibility of such changes in relative humidity, however, since the present study itself suggests that relative humidity remained fairly constant around 70% throughout the last 20,000 years.

Temporal variability seems more dramatic in δ_M than in S_M. Relative to the present, reversed Atlantic-Mediterranean $\delta^{18}O$ gradients may occur, while salinity gradients remain similar to the present, albeit weakened. The nonproportionality between δ_M and S_M responses to forcing by an internally consistent set of environmental change is found to be highly variable with time. Also, temporal S:$\delta^{18}O$ gradients are found to be significantly different from spatial gradients on the modeled timescales. This seriously limits the quality of Mediterranean paleosalinity

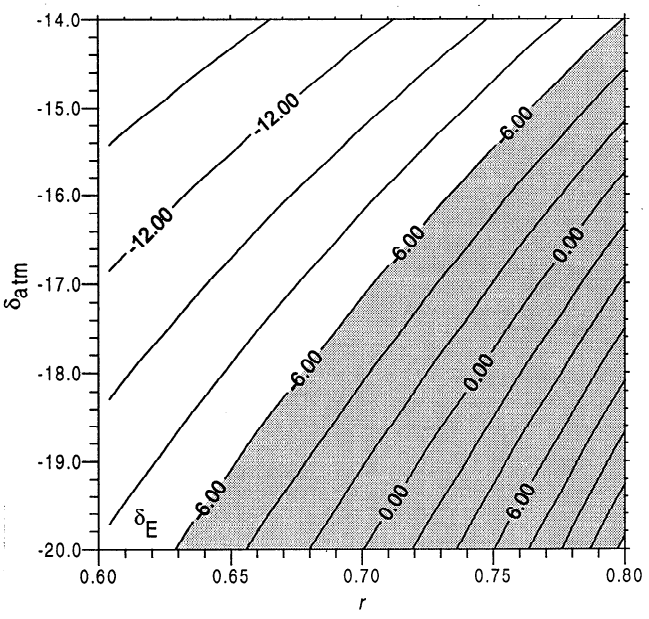

Figure 7. Surface plot for δ_E^{crit} (section 4.1) as a function of atmospheric $\delta^{18}O$ (δ_{atm}) and relative humidity r. Shading indicates zone where δ_E^{crit} is less depleted than −6‰.

reconstructions based on oxygen isotope residuals; it is likely that the associated error margins would be larger than the inferred paleosalinity changes. However, oxygen isotope residuals may still play a pivotal role in studies of (paleo)circulation. This potential may be unlocked by allowing (coupled) circulation models to advect oxygen isotopes through the system as a passive, nondynamic tracer. Validation of simulated isotope residual distributions, using observed distribution patterns, then provides valuable insight into the quality of modeled advection and mixing and therefore circulation.

Acknowledgments. I thank G.R. Bigg, N.J. Wells, P. Myers, K. Haines, H. Bryden, and J. Thomson for valuable suggestions, S.R. Troelstra for the T26B isotope data, and G. Schmidt and R. Zahn for constructive reviews. This paper contributes to EC-MAST3 program CLIVAMP (MAS3-CT95-0043) and Leverhulme Trust project "Oxygen isotopes: disentangling a record of oceanic and atmospheric variability" (F/204/Q).

References

Abbott, P.F., and R.C. Tabony, The estimation of humidity parameters, *Meteorol. Mag., 114*, 49-56, 1985.

Adamson, D.A., F. Gasse, F.A. Street, and M.A.J. Williams, Late Quaternary history of the Nile, *Nature, 288*, 50-55, 1980.

Aksu, A.E., D. Yaşar, P.J. Mudie, and H. Gillespie, Late glacial-Holocene paleoclimatic and paleoceanographic evolution of the Aegean Sea: Micropaleontological and stable isotopic evidence, *Mar. Micropaleontol., 25*, 1-28, 1995.

Arthur, M.A., and W.E. Dean, Ogranic-matter production and preservation and evolution of anoxia in the Holocene Black Sea, *Paleoceanography, 13*, 395-411, 1998.

Bar-Matthews, M., A. Ayalon, and A. Kaufman, Late Quaternary climate in the eastern Mediterranean region—Inferences from the stable isotope systematics of speleothems of the Soreq cave (Israel), *Quat. Res., 47*, 155-168, 1997.

Bar-Matthews, M., A. Ayalon, A. Kaufman, and G.J. Wasserburg, The eastern Mediterranean paleoclimate as a reflection of regional events: Soreq cave, Israel, *Earth Planet. Sci. Lett., 166*, 85-95, 1999.

Béthoux, J.P., Paléo-hydrologie de la Méditerranée au cours des derniers 20 000 ans, *Oceanol. Acta, 7*, 43-48, 1984.

Bigg, G.R., An ocean general circulation model view of the glacial Mediterranean thermohaline circulation, *Paleoceanography, 9*, 705-722, 1994.

Bigg, G.R., Aridity of the Mediterranean Sea at the last glacial maximum: A reinterpretation of the $\delta^{18}O$ record, *Paleoceanography, 10*, 283-290, 1995.

Bryden, H.L., and T.H. Kinder, Steady two-layer exchange through the Strait of Gibraltar, *Deep Sea Res., Part A, 38* (suppl. 1), s445-s463, 1991.

Bryden, H.L., J. Candela, and T.H. Kinder, Exchange through the Strait of Gibraltar, *Prog. Oceanogr., 33*, 201-248, 1994.

Cita, M.B., C. Vergnaud-Grazzini, C. Robert, H. Chamley, N. Ciaranfi, and S. d'Onofrio, Paleoclimatic record of a long deep sea core from the eastern Mediterranean, *Quat. Res., 8*, 205-235, 1977.

Coplen, T.B., C. Kendall, and J. Hopple, Comparison of stable isotope reference samples, *Nature, 302*, 236-238, 1983.

CLIMAP, The last interglacial ocean, *Quat. Res., 21*, 123-224, 1984.

Craig, H., and L.I. Gordon, Isotope oceanography: Deuterium and oxygen 18 variations in the ocean and the marine atmosphere, *Occas. Publ. 3*, pp. 277-374, Univ. Rhode Island, Kingston, 1965.

Dong, B., and P.J. Valdes, Sensitivity studies of northern hemisphere glaciation using an atmospheric GCM, *J. Clim., 8*, 2471-2496, 1995.

Duplessy, J.C., L. Labeyrie, A. Juillet-Leclerc, F. Maître, J. Duprat, and M. Sarnthein, Surface salinity reconstruction of the North Atlantic Ocean during the last glacial maximum, *Oceanol. Acta, 14*, 311-324, 1991.

Fairbanks, R.G., A 17,000-year glacio-eustatic sea level record: Influence of glacial melting rates on the Younger Dryas event and deep-ocean circulation, *Nature, 342*, 637-642, 1989.

Fairbanks, R.G., The age and origin of the "Younger Dryas Climate Event" in Greenland ice cores, *Paleoceanography, 5*, 937-948, 1990.

Fontugne, M.R., and S.E. Calvert, Late Pleistocene variability of the carbon isotopic composition of organic matter in the eastern Mediterranean: Monitor of changes in carbon sources and atmospheric CO_2 concentrations, *Paleoceanography, 7*, 1-20, 1992.

Garrett, C., R. Outerbridge, and K. Thompson, Interannual variability in Mediterranean heat budget and buoyancy fluxes, *J. Clim., 6*, 900-910, 1993.

Gat, J.R., Oxygen and hydrogen isotopes in the hydrologic cycle, *Annu. Rev. Earth Planet. Sci., 24*, 225-262, 1996.

Gonfiantini, R., Environmental isotopes in lake studies, in *Handbook of Environmental Isotope Geochemistry*, Vol. 2, edited by P. Fritz and J.C. Fontes, pp. 113-168, Elsevier, New York, 1986.

Goodfriend, G.A., Holocene trends in ^{18}O in snail shells from the Negev desert and their implications for changes in rainfall source areas, *Quat. Res., 35*, 417-426, 1991.

Gorshkov, S.G. (ed.), *World Ocean Atlas*, Vol. 2, *Atlantic and Indian Oceans*, 306 pp., Pergamon, Tarrytown, N. Y., 1978.

Guiot, J., A. Pons, J.L. de Beaulieu, and M. Reille, A 140,000-year continental climate reconstruction from two European pollen records, *Nature, 338*, 309-313, 1989.

Hemleben, C, D. Meischner, R. Zahn, A. Almogi-Labin, H. Erlenkeuser, and B. Hiller, Three hunderd eighty thousand year long stable isotope and faunal records from the Red Sea: Influence of global sea level change on hydrography, *Paleoceanography, 11*, 147-156, 1996.

Higgs, N.C., J. Thomson, T.R.S. Wilson, and I.W. Croudace, Modification and complete removal of eastern Mediterranean sapropels by postdepositional oxidation, *Geology, 22*, 423-426, 1994.

Hilgen, F.J., Astronomical calibration of Gauss to Matuyama sapropels in the Mediterranean and implication for the geomagnetic Polarity Time Scale, *Earth Planet. Sci. Lett., 104*, 226-244, 1991.

Hoffmann, G., and M. Heimann, Water isotope modeling in the Asian monsoon region, *Quat. Int., 37*, 115-128, 1997.

Joussaume, S., and J. Jouzel, Paleoclimatic tracers: An investigation using an atmospheric general circulation model under ice age conditions, 2, water isotopes, *J. Geophys. Res., 98*, 2807-2830, 1993.

Jouzel, J., C. Lorius, J.R. Petit, C. Genthon, N.I. Barkov, V.M. Kotlyakov, and V.M. Petrov, Vostok ice core: A continuous isotope temperature record over the last climatic cycle (160,000 years), *Nature, 329*, 403-408, 1987.

Kallel, N., M. Paterne, J.C. Duplessy, C. Vergnaud-Grazzini, C. Pujol., L.D. Labeyrie, M. Arnold, M. Fontugne, and C. Pierre, Enhanced rainfall in the Mediterranean region during the last sapropel event, *Oceanol. Acta, 20*, 697-712, 1997a.

Kallel, N., M. Paterne, L. Labeyrie, J.C. Duplessy, and M. Arnold, Temperature and salinity records of the Tyrrhenian Sea during the last 18,000 years, *Palaeogeogr. Palaeoclimatol. Palaeoecol., 135*, 97-108, 1997b.

Klein, R., Y. Loya, G. Gvirtzman, P.J. Isdale, and M. Susic, Seasonal rainfall in the Sinai Desert during the late Quaternary inferred from fluorescent bands in fossil corals, *Nature, 345*, 145-147, 1990.

Kutzbach, J.E., P.J. Guetter, P.J. Behling, and R. Selin, Simulated climatic changes: Results of the COHMAP climate-model experiments, in *Global Climates Since the Last Glacial Maximum*, edited by H.E. Wright, Jr. et al., pp. 24-93, Univ. of Minn. Press, Minneapolis, 1993.

Labeyrie, L.D., J.C. Duplessy, and P.L. Blanc, Variations in the mode of formation and temperature of oceanic deep waters over the past 125,000 years, *Nature, 327*, 477-482, 1987.

Lane-Serff, G.F., E.J. Rohling, H.L. Bryden, and H. Charnock, Postglacial connection of the Black Sea to the Mediterranean and its relation to the timing of sapropel formation, *Paleoceanography, 12*, 169-174, 1997.

Majoube, M., Fractionnement en oxygène 18 et deuterium entre l'eau et sa vapeur, *J. Chim. Phys., 10*, 1423-1436, 1971.

Maslin, M.A., N.J. Shackleton, and U. Pflaumann, Surface water temperature, salinity, and density changes in the northeast Atlantic during the last 45,000 years: Heinrich events, deep water formation, and climatic rebounds, *Paleoceanography, 10*, 527-544, 1995.

McKenzie, J.A., Pluvial conditions in the eastern Sahara following the penultimate deglaciation: Implications for changes in atmospheric circulation patterns with global warming, *Palaeogeogr. Palaeoclimatol. Palaeoecol., 103*, 95-105, 1993.

Merlivat, L., and J. Jouzel, Global climatic interpretation of the deuterium-oxygen 18 relationship for precipitation, *J. Geophys. Res., 84*, 5029-5033, 1979.

Myers, P., K. Haines, and E.J. Rohling, Modeling the paleocirculation of the Mediterranean: The last glacial maximum and the Holocene with emphasis on the formation of sapropel S1, *Paleoceanography, 13*, 586-606, 1998.

National Institute of Standards and Technology, *Report of Investigation, Reference Materials*, pp. 8543-8546, Gaithersburgh, Md., 1992.

Naval Oceanography Command Detachment, Asheville, N. C., *U.S. Navy Marine Climatic Atlas of the World, Vol. IX, World-Wide Means and Standard Deviations*, U.S. Gov. print. off., Washington, D. C., 1981.

Oguz, T., E. Orzoy, M.A. Latif, H.I. Sur, and U. Unlüata, Modeling of hydraulically controlled exchange flow in the Bosporus Strait, *J. Phys. Oceanogr., 20*, 945-965, 1990.

O'Neil, J.R., R.N. Clayton, and T.K. Mayeda, Oxygen isotope fractionation on divalent metal carbonates, *J. Chem. Phys., 51*, 5547-5558, 1969.

Pierre, C., The oxygen and carbon isotope distribution in the Mediterranean water masses, *Mar. Geol., 153*, 41-55, 1999.

Pujol, C., and C. Vergnaud-Grazzini, Palaeoceanography of the last deglaciation in the Alboran Sea (western Mediterranean), stable isotopes and

planktonic foraminiferal records, *Mar. Micropaleontol., 15*, 153-179, 1989.

Reichart, G.J., L.J. Lourens, and W.J. Zachariasse, Temporal variability in the northern Arabian Sea Oxygen Minimum Zone (OMZ) during the last 225,000 years, *Paleoceanography, 13*, 607-621, 1998.

Rohling, E.J., Review and new aspects concerning the formation of Mediterranean sapropels, *Mar. Geol., 122*, 1-28, 1994.

Rohling, E.J., and G.R. Bigg, Paleosalinity and $\delta^{18}O$: A critical assessment, *J. Geophys. Res., 103*, 1307-1318, 1998.

Rohling, E.J., and H.L. Bryden, Estimating past changes in the eastern Mediterranean freshwater budget, using reconstructions of sea level and hydrography, *Proc. K. Ned. Akad. Wet. Biol. Chem. Geol. Phys. Med. Sci., 97*, 201-217, 1994.

Rohling, E.J., and S. De Rijk, The Holocene Climate Optimum and Last Glacial Maximum in the Mediterranean: The marine oxygen isotope record, *Mar. Geol., 153*, 57-75, 1999.

Rohling, E.J., and F.J. Hilgen, The eastern Mediterranean climate at times of sapropel formation: A review, *Geol. Mijnbouw, 70*, 253-264, 1991.

Rohling, E.J., M. Den Dulk, C. Pujol, and C. Vergnaud-Grazzini, Abrupt hydrographic change in the Alboran Sea (western Mediterranean) around 8000 yrs BP, *Deep Sea Res., Part 1, 42*, 1609-1619, 1995.

Rohling, E.J., F.J. Jorissen, C. Vergnaud-Grazzini, and W.J. Zachariasse, Northern Levantine and Adriatic planktonic foraminifera: Reconstruction of paleoenvironmental gradients, *Mar. Micropaleontol., 21*, 191-218, 1993.

Rohling, E.J., F.J. Jorissen, and H.C. De Stigter, 200 year interruption of Holocene sapropel formation in the Adriatic Sea. *J. Micropalaeontol., 16*, 97-108, 1997.

Rohling, E.J., A. Hayes, S. De Rijk, D. Kroon, J.W. Zachariasse, and D. Eisma, Abrupt cold spells in the northwest Mediterranean, *Paleoceanography, 13*, 316-322, 1998.

Rossignol-Strick, M., Rainy periods and bottom water stagnation initiating brine accumulation and metal concentrations, 1, the late Quaternary, *Paleoceanography, 2*, 333-360, 1987.

Rossignol-Strick, M., V. Nesteroff, P. Olive, and C. Vergnaud-Grazzini, After the deluge: Mediterranean stagnation and sapropel formation, *Nature, 295*, 105-110, 1982.

Rozanski, K., Deuterium and oxygen-18 in European groundwaters—Links to atmospheric circulation in the past, *Chem. Geol., 52*, 349-363, 1985.

Rozanski, K., C. Sonntag, and K.O. Münnich, Factors controlling stable isotope composition of European precipitation, *Tellus, 34*, 142-150, 1982.

Rozanski, K., L. Araguás-Araguás, and R. Gonfiantini, Isotopic patterns in modern global precipitation, in *Climate Change in Continental Isotopic Records, Geophys. Monogr. Ser.*, Vol. 78, edited by P.K. Swart et al., pp. 1-36, AGU, Washington, D. C., 1993.

Ryan, W.B.F., W.C. Pittman III, C.O. Major, K. Shimkus, V. Moskalenko, G.A. Jones, P. Dimitrov, N. Gorür, M. Sakinç, and H. Yüce, An abrupt drowning of the Black Sea shelf, *Mar. Geol., 138*, 119-126, 1997.

Schmidt, G.A., Oxygen-18 variations in a global ocean model, *Geophys. Res. Lett., 25*, 1201-1204, 1998.

Schrag, D.P., G. Hampt, and D.W. Murray, Pore fluid constraints on the temperature and oxygen isotopic composition of the glacial ocean, *Science, 272*, 1930-1932, 1996.

Shackleton, N.J., Oxygen isotopes, ice volume and sea-level, *Quat. Sci. Rev., 6*, 183-190, 1987.

Shaw, H.F., and G. Evans, The nature, distribution and origin of a sapropelic layer in sediments of the Cilicia Basin, northeastern Mediterranean, *Mar. Geol., 61*, 1-12, 1984.

Sonntag, C., E. Klitzsch, E.P. Löhnert, E.M. El Shazly, K.O. Münnich, Ch. Junghans, U. Thorweihe, K. Weistroffer, and F.M. Swailem, Paleoclimatic information from deuterium and oxygen-18 in carbon-14-dated north Saharan groundwaters, in *Isotope Hydrology 1978*, Vol. II, pp. 569-580, Int. At. Energy Agency, Vienna, 1979.

Stanev, E.V., H.J. Friedrich, and S.V. Botev, On the seasonal response of intermediate and deep water to surface forcing in the Mediterranean Sea, *Oceanol. Acta, 12*, 141-149, 1989.

Street, A.F., and A.T. Grove, Global maps of lake-level fluctuations since 30,000 YBP, *Quat. Res., 12*, 83-118, 1979.

Sultan, M., N. Sturchio, F.A. Hassan, M.A.R. Hamdan, A.M. Mahmood, Z. El Alfy, and T. Stein, Precipitation source inferred from stable isotopic composition of Pleistocene groundwater and carbonate deposits in the western desert of Egypt, *Quat. Res., 48*, 29-37, 1997.

Swart, P.K., The oxygen and hydrogen isotopic composition of the Black Sea, *Deep Sea Res., Part A, 38*, suppl. 2, s761-s772, 1991.

Thomson, J., N.C. Higgs, T.R.S. Wilson, I.W. Croudace, G.J. De Lange, and P.J.M. Van Santvoort, Redistribution and geochemical behaviour of redox-sensitive elements around S1, the most recent eastern Mediterranean sapropel, *Geochim. Cosmochim. Acta., 59*, 3487-3501, 1995.

Thunell, R.C., and D.F. Williams, Glacial-Holocene salinity changes in the Mediterranean Sea: Hydrographic and depositional effects, *Nature, 338*, 493-496, 1989.

Tolmazin, D., Changing coastal oceanography of the Black Sea, I, Northwestern shelf, *Prog. Oceanogr., 15*, 217-276, 1985.

Troelstra, S.R., G.M. Ganssen, K. Van der Borg, and A.F.M. De Jong, A late Quaternary stratigraphic framework for eastern Mediterranean sapropel S1 based on AMS ^{14}C dates and stable oxygen isotopes, *Radiocarbon, 33*, 15-21, 1991.

Vergnaud-Grazzini, C. Mediterranean late Cenozoic stable isotope record: stratigraphic and paleoclimatic implications, in *Geological evolution of the Mediterranean Basin*, edited by D.J. Stanley and F.C. Wezel, pp. 413-451, Springer-Verlag, New York, 1985.

Vergnaud-Grazzini, C., W.B.F. Ryan, and M.B. Cita, Stable isotope fractionation, climatic change and episodic stagnation in the eastern Mediterranean during the late Quaternary, *Mar. Micropaleontol., 2*, 353-370, 1977.

Wang, L., M. Sarnthein, J.C. Duplessy, H. Erlenkeuser, S. Jung, and U. Pflaumann, Paleo sea surface salinities in the low-latitude Atlantic: The $\delta^{18}O$ record of *Globigerinoides ruber* (white), *Paleoceanography, 10*, 749-761, 1995.

Wells, N.C., *The Atmosphere and Ocean: a Physical Introduction*, 347 pp., Taylor and Francis, Bristol, Pa., 1986.

Wells, N.C., Surface heat fluxes in the western equatorial Pacific Ocean, *Ann. Geophys., 13*, 1047-1053, 1995.

Wells, N.C., and S. King-Hele, Parameterization of tropical ocean heat flux, *Q. J. R. Meteorol. Soc., 116*, 1213-1224, 1990.

Wijmstra, T.A., R. Young, and H.J.L. Witte, An evaluation of the climatic conditions during the late Quaternary in northern Greece by means of multivariate analysis of palynological data and comparison with recent phytosociological and climatic data, *Geol. Mijnbouw, 69*, 243-251, 1990.

E.J. Rohling, School of Ocean and Earth Science, Southampton University, Southampton Oceanography Centre, Waterfront Campus, European way, Southampton SO14 3ZH, England (E.Rohling@soc.soton.ac.uk)

(Received April 15, 1999;
revised July 6, 1999;
accepted July 20, 1999.)